

Fabrication of Conductive Nanoporous Membranes using Self-Assembling Block Copolymers for Electrically Controlled Diffusive Flow

Ece Isenbike Ozalp, Sungho Kim, Vignesh Sundar, Jian-Gang (Jimmy) Zhu, and Jeffrey A. Weldon

Carnegie Mellon University, Pittsburgh, PA, USA, eozalp@andrew.cmu.edu

ABSTRACT

This paper reports on the fabrication of an intrinsically conductive nanoporous membrane with high pore density (10^{11} pores per cm^2) using self-assembling block copolymers which has the potential to enable the controlled diffusion of charged molecules via the exclusion-enrichment effect, with potential applications in drug-delivery. Finite element simulations of an electrically gated nanochannel indicate the possibility to alter the diffusion rate of molecules through the membrane by several orders of magnitude using a ± 1 gate voltage. The nanochannels with 25 nm diameter pore size were fabricated into an amorphous silicon thin film sheathed by native oxide in order to enable gating. Poly (styrene-*b*-dimethyl siloxane) block copolymer was first used to generate a highly dense array of pillars; the pattern was then reversed and subsequently transferred into the amorphous silicon thin film.

Keywords: Nanoporous membrane, drug delivery, block copolymer, nanofluidics.

1 INTRODUCTION

Nanoporous membranes have been widely investigated due to high demand for biological applications such as bio-sensing, filtration and drug-delivery[1]–[3]. Their properties such as small pore size and high surface-to-volume ratio make them applicable for nanofluidic applications via controlled diffusion due to the comparable sizes between the charged molecules and the nanochannels[4]. Such membranes can be fabricated using lithography, anodization of aluminium or titanium, or block copolymers[5]–[7].

In the application of the majority of previously reported nanoporous membranes, the diffusion rate is primarily determined by the pore size[8]–[10]. As a result, the diffusion rate is fixed for a given fabrication process. It has been shown that channel electrical potential can modify the diffusion rate of charged molecules[11]. Therefore, if the electrical potential in the nanochannel can be externally manipulated, transport of charged molecules through the membrane can be actively controlled[12]. Karnik et al.[6] developed a nanofluidic transistor structure that uses a gate electrode on nanofluidic channels to control the surface charge and therefore modulate the flow using field-effect control. However, these devices were fabricated as a planar structure, and the fabrication process is not suitable for

membrane structures. A conductive membrane with an insulating layer would allow electrical gating thereby enabling the control of the diffusion of charged molecules. Many molecules of interest, including drug molecules and proteins, are charged and thus lend themselves to control through electrical gating.

Conductive nanoporous membranes potentially allow for external electrical control of the transport behavior through the nanochannels via the exclusion-enrichment effect when the diameter of the channel is comparable to the electrical double layer (EDL) thickness [12], [13]. For the fabrication of such membranes, e-beam lithography and focused ion beam (FIB)-based processes can allow great deal of control when it comes to pore sizes, shapes and the position of the pores; however, they cannot be used for large areas due to the high cost and long fabrication time[14]. Anodic aluminum oxide (AAO) membranes have been widely used in the fabrication of nanoporous membranes. These membranes have many desirable properties some of which are biocompatibility, small pore size and uniformity[5], [8]. Pore diameter for AAO membranes can vary from 2-300 nm, and pore density is in the range of 10^9 - 10^{11} pores/ cm^2 . Pore size can be controlled using applied voltage, reaction time, etc.[7], [15] However, the anodization process converts the aluminum to alumina which is electrically insulating. Wu et al.[16] transferred the pattern of nanoporous anodic aluminum oxide membrane into a tungsten thin film, and then oxidized the tungsten surface to form a dielectric layer. However, pattern transfer of AAO membrane into a tungsten film significantly reduced the pore density. Pardon et al. [17] used atomic layer deposition techniques to deposit platinum and aluminum oxide dual layer on top of AAO membranes to create a metal-insulator stack inside the nanopore. However, to electrically gate with minimal gate leakage current, a pinhole free oxide layer is necessary, which is difficult to achieve unless the insulating layer is sufficiently thick. Deposition of the insulating layer is further complicated by the nanoporous structure of these membranes.

Our fabrication process is fundamentally different; the membrane is intrinsically conductive. Block copolymers are used to fabricate the initial pattern of our membrane structure. Block copolymers (BCPs) can be used to fabricate patterns with higher pore densities ($> 10^{11}$ per cm^2) with a uniform, narrow pore size, pore shape and size tunability by changing the molecular weights and composition, making them a very desirable material to use[2], [18]. The pore size

(~25 nm) and pore density ($\sim 10^{11}$ pores cm^{-2}) in the membrane is inherent and does not change throughout the process. Therefore, the pore density of the final membrane is still as high as that of block copolymer patterns. Further, the optimal channel size required to provide high diffusion rate and low voltage electrical control, as indicated in simulations, can be achieved using block copolymers, while still maintaining a high pore density.

2 SIMULATIONS

In our previous work, we modeled the effect of membrane potential on the diffusion of charged molecules through silicon/silica nanochannels. We demonstrated through simulation that cylindrical nanochannel structures with chemically treated surfaces have the ability to control the diffusive transport with a small applied DC gate voltage[12]. If the diameter of the nanochannel gets too small comparable to the drug molecule, single file diffusion behavior occurs limiting the overall diffusion rate. Conversely, channel diameters larger than 100 nm require an unrealistically high control voltage. To predict the controllability of the fabricated nanoporous membrane structure, we analyzed gated molecular diffusion through simulation in nanochannels with 25 nm in diameter and 50nm in length between two chambers with asymmetric concentrations of charged drug molecules. The modeled drug molecules INF α -2b and leuprolide, which are used for the cancer treatment, have -2 and +1 net formal charges, respectively[24]. The gated nanochannel structures were modeled in the finite element software COMSOL Multiphysics. The simulation results are shown in figure 1. Simulation result shows the relative drug molecule flux flowing through the nanochannel structure with controlled gate voltage. For positively charged drug molecule, Leuprolide, flux is increased with the negative gate voltage and decreased by the positive gate voltage. For negatively charged molecule, opposite behavior is observed. This result indicates that the nanochannel with 25 nm diameter can alter the diffusion rate by many orders of magnitude under certain conditions with a ± 1 volt gate voltage.

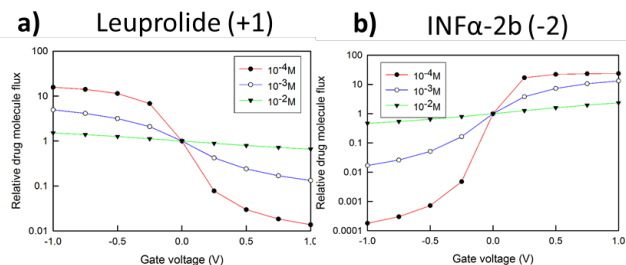


Figure 1 Simulated diffusive transport flux of **a)** Leuprolide (formal charge: +1) and **b)** INF α -2b (formal charge: -2) measured at the end of the nanochannel. Note that the y axis is log scale.

3 FABRICATION METHODS

A 50 nm thin film of amorphous silicon (am-Si) was sputter deposited with an argon pressure of 5 mT at the rate of 0.1 nm per second. The resistivity of the resulting thin film was measured using the 4 point probe method to be 40 ohm-m. A thin layer of native silicon dioxide was used to enable the gating of the device. While the conductivity of amorphous silicon is lower than metals, it can be patterned using fluoride-based plasmas in a reactive ion etching system. Using a bias voltage, anisotropic etch profiles can be achieved, enabling high-aspect ratio patterning into the membrane layer.

Block copolymers, which are comprised of two blocks of different polymers connected by a covalent bond, have attracted extensive research over the last few years due to their self-assembly characteristics. These have been used to form both periodic and aperiodic nanostructures for semiconductor and data storage applications[19]. Diblock copolymer poly styrene-b-dimethyl siloxane (PS-b-PDMS) was used in this work. The two blocks in this polymer have a high enthalpy of mixing, as indicated by its relatively high Flory-Huggins interaction parameter (χ) of 0.26[20]. Based on the high Flory-Huggins interaction parameter, PS-b-PDMS is more promising for small scale fabrication compared to other polymers such as PS-PMMA ($\chi \sim 0.04$ -0.06)[20]. Using PS-b-PDMS with a molecular weight of 51 kg/mol and 17 vol% PDMS, a regular array of PDMS spheres in a polystyrene matrix can be obtained, with a center-to-center distance of 35 nm between the PDMS spheres as shown in the plane-view scanning electron micrograph, figure 2. Further, the polystyrene block (which consists of a carbon-like backbone) etches much faster in an oxygen plasma in a reactive ion etching process compared to PDMS (which consists of a silicon-like backbone), enabling pattern transfer into the underlying mask structure[20].

Figure 3 illustrates the process flow for the fabrication of amorphous silicon membranes using block copolymer nanostructures as the initial pattern. An array of PDMS dots (from the PS-b-PDMS block copolymer thin film) was used as an etch mask to pattern an array of pillars into a suitable mask structure. The pattern was then reversed using a spin-on-glass, and subsequently transferred into the am-Si layer.

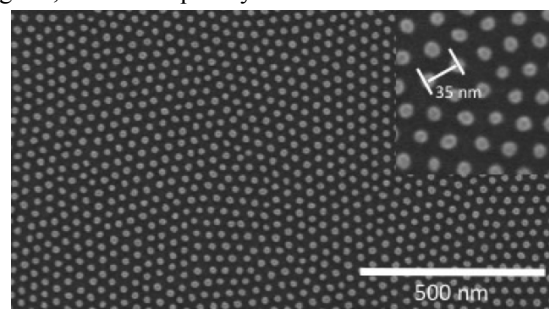


Figure 2 Scanning electron microscopy (SEM) image of block copolymer pattern

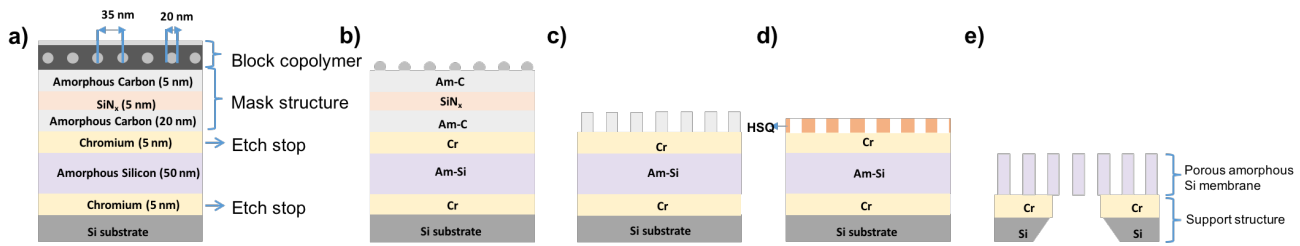


Figure 3 Schematics process flow of the fabrication of the conductive nanoporous membrane at the wafer scale. **a)** Initial film stack **b)** After block copolymer etch **c)** After amorphous carbon pillar fabrication **d)** After reverse patterning using spin on glass (HSQ) **e)** After pattern transfer into 50 nm thick amorphous silicon layer and releasing the membrane

The initial film stack (shown in Figure 3a) consists of the mask structure (for carbon pillar fabrication and pattern reversal), the am-Si membrane layer and an etch stop layer of chromium sputtered onto a single crystal silicon substrate (with native oxide intact).

PS-*b*-PDMS, as purchased from Polymer Source Inc. was diluted (0.08 g in 10 ml) in a toluene solution. A thin film was deposited onto the film stack using a Solitec spin coating system using the dynamic dispense technique (spread parameters: 600 rpm, 6 sec; spin parameters: 4000 rpm, 60 sec). The concentration and spin conditions were optimized so that one monolayer of PDMS spheres in a PS matrix was obtained. Thermal annealing for 24 hours at 175 °C was performed to facilitate the micro-phase separation process (Figure 2). A CF₄ plasma was first utilized to etch the PDMS film that segregated to the polymer-air interface in a PlasmaTherm 790 RIE system[21]. A low-bias oxygen plasma was then used to selectively etch the PS matrix exposing an array of PDMS spheres. This pattern can then be

transferred using a second oxygen plasma into the underlying mask structure.

The mask structure comprised of layers of amorphous carbon (am-C) (5 nm), silicon nitride (5 nm) and a thicker amorphous carbon layer (20 nm). Alternating thin layers of am-C and silicon nitride are necessary to obtain pattern with desired height and vertical side-walls due to their contrasting etch-chemistries. Alternating oxygen and CF₄ plasmas were utilized to transfer the pattern from the PDMS dots to the final thick am-C layer (shown in Figure 3c). Without these intermediate layers, the pattern transfer into the 20 nm am-C layer is incomplete. This is because physical erosion component during the RIE process affects the PDMS spheres more than it affects the silicon nitride.

In order to reverse the pattern, hydrogen-silsesquioxane (HSQ), which is a commonly used negative e-beam resist and a spin-on-glass, was utilized. The HSQ was dispensed onto the sample by spin-coating (spread parameters: 600 rpm, 4 sec; spin parameters: 4000 rpm, 60 sec) then baked at 180°C for 1 minute. Upon baking, the HSQ molecules cross-link, forming a network structure similar to silicon dioxide (SiO₂)[22]. To reverse the pattern, the thickness of the HSQ layer was needed to be much higher than the height of the fabricated pillars, resulting in a nearly planar surface, as shown by the SEM image in Figure 4b. HSQ has been used for planarization in the semiconductor industry[22], and since it is spin coated from a solution, fills the gaps between the pillars as well. Since the properties of the baked HSQ are similar to SiO₂ it can be etched using a CF₄ plasma in RIE. This was done until the tops of the am-C pillars were exposed, as shown in Figure 4c. Then, using an O₂ plasma (which does not etch the HSQ), the am-C pillars were etched away, and thus a negative of the previous pattern was created, as seen from the plane-view scanning electron micrograph in Figure 4d. The HSQ alone is insufficient for the final pattern transfer step into the am-Si membrane layer, since their etch rates in a fluoride plasma are similar. Thus, the HSQ pattern was first transferred to a thin 5 nm chromium layer using a chlorine plasma in a Plasma Therm Versaline ICP RIE system, and then finally to the 50 nm thick am-Si membrane layer using a CF₄ plasma.

To release the membrane, 50 micron windows were patterned using photolithography on the reverse-side of the single crystal silicon substrate. The reverse-side was then

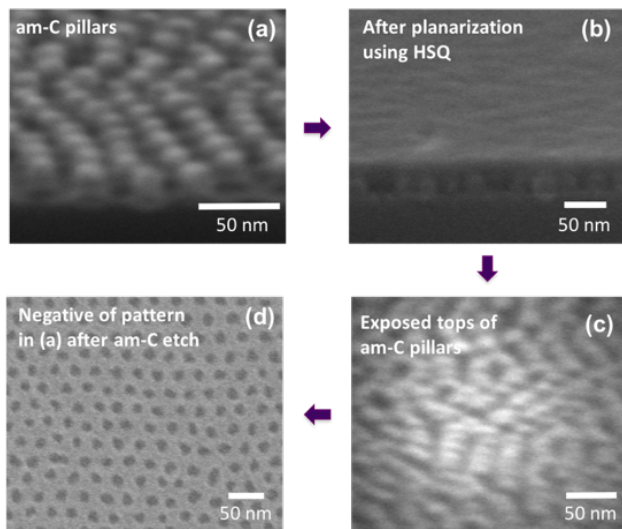


Figure 4 SEM images of **a)** tilt-view image of amorphous carbon pillars after pattern transfer **b)** tilt-view image after spin coating HSQ **c)** tilt-view image of etch back to expose the tops of amorphous carbon pillars and **d)** after removal of amorphous carbon pillars

exposed to XeF₂ vapor in a vapor-phase etching system, etching the silicon of the wafer in an isotropic fashion. A thin 5 nm layer of Cr between the membrane-side and the reverse-side served as the etch-stop to protect the membrane. Once the membrane release was complete, this Cr layer was removed using chlorine plasma as described earlier.

Figure 5 shows a tilt-view scanning electron micrograph of the high pore density amorphous silicon nanoporous membrane with vertical sidewalls. For electrical gating of the membrane, a conformal insulating layer is necessary. The insulating layer in this case does not require an additional deposition, because amorphous silicon can be oxidized to form a pinhole free insulating layer[23]. Furthermore, any damage to the oxide layer will self-heal due to the oxidation of the underlying amorphous silicon structure.

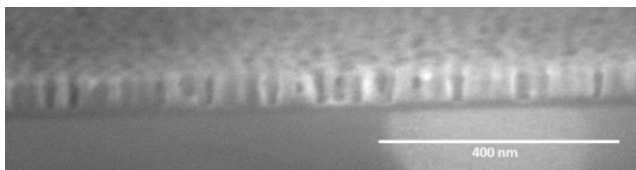


Figure 5 SEM tilt view of amorphous silicon membrane

4 CONCLUSION

We have fabricated a gateable highly porous (10^{11} pores cm^{-2}) intrinsically conductive membrane structures with ~ 25 nm pore diameters. The channel dimension was determined by modelling the gated diffusion through the nanochannel. The simulation results show that the nanochannel with 25 nm diameter can alter the molecular diffusion rate of drug molecules with a ± 1 volt gate voltage. To fabricate our intrinsically conductive highly nanoporous membrane structure, PS-b-PDMS was used to pattern the nanochannels. The pattern of BCP then was transferred to a mask structure. Once the pillar structure is achieved, the sample is covered with spin-on glass for reverse patterning. Amorphous silicon is etched to get the porous structure and then the membrane is released using XeF₂. Overall, this novel structure allows for self-healing, gateable, high pore density intrinsically conductive nanoporous membrane that enables the controlled diffusion of the charged molecules.

Acknowledgments

This project was funded by through the CMU-SYSU Collaborative Innovation Research Center (CIRC) of Carnegie Mellon University. The authors would like to thank Dr. Matthew Moneck, executive manager of Carnegie Mellon University Nanofabrication Facility.

5 REFERENCES

- [1] D. A. Bernards and T. A. Desai, *Adv. Mater.*, vol. 22, no. 21, pp. 2358–2362, 2010.
- [2] E. A. Jackson and M. A. Hillmyer, *ACS Nano*, vol. 4, no. 7, pp. 3548–3553, 2010.
- [3] T. A. Desai, D. J. Hansford, L. Leoni, M. Essenpreis, and M. Ferrari, *Biosens. Bioelectron.*, vol. 15, no. 9–10, pp. 453–462, 2000.
- [4] R. B. Schoch, J. Han, and P. Renaud, *Rev. Mod. Phys.*, vol. 80, no. 3, pp. 839–883, 2008.
- [5] E. Gultepe, D. Nagesha, S. Sridhar, and M. Amiji, *Adv. Drug Deliv. Rev.*, vol. 62, no. 3, pp. 305–315, 2010.
- [6] R. Karnik, K. Castelino, and A. Majumdar, *Appl. Phys. Lett.*, vol. 88, no. 12, pp. 1–4, 2006.
- [7] P. Stroeve and N. Ileri, *Trends Biotechnol.*, vol. 29, no. 6, pp. 259–266, 2011.
- [8] C. Boss, E. Meurville, J. M. Sallese, and P. Ryser, *J. Memb. Sci.*, vol. 401–402, pp. 217–221, 2012.
- [9] L. Leoni, A. Boiarski, and T. A. Desai, *Biomed. Microdevices*, vol. 4, no. 2, pp. 131–139, 2002.
- [10] F. Montagne, N. Blondiaux, A. Bojko, and R. Pugin, *Nanoscale*, vol. 4, no. 19, p. 5880, 2012.
- [11] H. Daiguji, P. Yang, and A. Majumdar, p. 47405, 2004.
- [12] S. Kim, E. I. Ozalp, V. Sundar, J.-G. Zhu, and J. A. Weldon, *J. Appl. Phys.*, vol. 118, no. 7, p. 074301, 2015.
- [13] A. Plecis, R. B. Schoch, and P. Renaud, *Nano Lett.*, vol. 5, no. 6, pp. 1147–1155, 2005.
- [14] B. P. Nabar, Z. Çelik-Butler, B. H. Dennis, and R. E. Billo, *J. Micromechanics Microengineering*, vol. 22, no. 4, p. 045012, 2012.
- [15] K. Kim, M. Kim, and S. M. Cho, *Korean J. Chem. Eng.*, vol. 22, no. 5, pp. 789–792, 2005.
- [16] S. Wu, F. Wildhaber, A. Bertsch, J. Brugger, and P. Renaud, *Appl. Phys. Lett.*, vol. 102, no. 21, pp. 1–5, 2013.
- [17] G. Pardon, H. K. Gatty, G. Stemme, W. van der Wijngaart, and N. Roxhed, *Nanotechnology*, vol. 24, no. 1, p. 015602, 2013.
- [18] S. Y. Yang, J. A. Yang, E. S. Kim, G. Jeon, E. J. Oh, K. Y. Choi, S. K. Hahn, and J. K. Kim, *ACS Nano*, vol. 4, no. 7, pp. 3817–3822, 2010.
- [19] M. P. Stoykovich and P. F. Nealey, *Mater. Today*, vol. 9, no. 9, pp. 20–29, 2006.
- [20] C. Cummins, A. Gangnaik, R. A. Kelly, D. Borah, J. O. Connell, N. Petkov, Y. M. Georgiev, J. D. Holmes, and M. A. Morris pp. 6712–6721, 2015.
- [21] Y. S. Jung and C. A. Ross, *Nano Lett.*, vol. 7, no. 7, pp. 2046–2050, 2007.
- [22] S. Choi, M. J. Word, V. Kumar, and I. Adesida, *J. Vac. Sci. Technol. B Microelectron. Nanom. Struct.*, vol. 26, no. 5, p. 1654, 2008.
- [23] F. Gaspard, A. Halimaoui, and G. Sarraeyrouse, *Rev. Phys. Appliquée*, vol. 22, no. 1, pp. 65–69, 1987.
- [24] A. Grattoni, H. Shen, D. Fine, A. Ziemys, J. S. Gill, L. Hudson, S. Hosali, R. Goodall, X. Liu, and M. Ferrari, *Pharm. Res.*, vol. 28, no. 2, pp. 292–300, 2011.